

# 1 Efficient and Flexible Integration of Variant Characteristics in Rare

## 2 Variant Association Studies Using Integrated Nested Laplace

### 3 Approximation

4 Hana Susak<sup>1,##a,##b</sup>, Laura Serra-Saurina<sup>2,##c,3</sup>, Raquel Rabionet Janssen<sup>1,##d</sup>, Laura Domènech<sup>1,2</sup>,  
5 Mattia Bosio<sup>1</sup>, Francesc Muyas<sup>1,##e</sup>, Xavier Estivill<sup>4</sup>, Georgia Escaramís<sup>1,2,##f\*¶</sup> and Stephan  
6 Ossowski<sup>1,5,##e¶</sup>

7 <sup>1</sup>Centre for Genomic Regulation (CRG), The Barcelona Institute of Science and Technology, Dr. Aiguader 88, 08003  
8 Barcelona, Spain.

9 <sup>2</sup>Biomedical Research Networking Centre consortium of Public Health and Epidemiology (CIBERESP).

10 <sup>3</sup>Center for research in occupational Health (CiSAL), Department of Experimental and Health Sciences, Universitat  
11 Pompeu Fabra, Barcelona, Spain.

12 <sup>4</sup>Women's Health Dexeus, Barcelona, Spain.

13 <sup>5</sup>Universitat Pompeu Fabra (UPF), Barcelona, Spain.

14 <sup>#a</sup>Current Address: Division of Computational Genomics and Systems Genetics, German Cancer Research Center  
15 (DKFZ), 69120 Heidelberg, Germany.

16 <sup>#b</sup>Current Address: European Molecular Biology Laboratory, Genome Biology Unit, 69117 Heidelberg, Germany.

17 <sup>#c</sup>Current Address: Research Group on Statistics, Econometrics and Health (GRECS), Universitat de Girona (UdG).

18 <sup>#d</sup>Current Address: Institut de Recerca Sant Joan de Déu; University of Barcelona, Barcelona, Spain.

19 <sup>#e</sup>Current address: Institute of Medical Genetics and Applied Genomics, University of Tübingen, Tübingen, Germany.

20 <sup>#f</sup>Departament de Biomedicina, Facultat de Medicina i Ciències de la Salut, Institut de Neurociències, Universitat de  
21 Barcelona, Spain

22

23 \*Corresponding author

24 E-mail: [gescaramis@ub.edu](mailto:gescaramis@ub.edu) (GE)

25

26 ¶These authors contributed equally to this work

## 27 Abstract

28 Rare variants are thought to play an important role in the etiology of complex diseases and may  
29 explain a significant fraction of the missing heritability in genetic disease studies. Next-  
30 generation sequencing facilitates the association of rare variants in coding or regulatory regions  
31 with complex diseases in large cohorts at genome-wide scale. However, rare variant association  
32 studies (RVAS) still lack power when cohorts are small to medium-sized and if genetic variation  
33 explains a small fraction of phenotypic variance. Here we present a novel Bayesian rare variant  
34 Association Test using Integrated Nested Laplace Approximation (BATI). Unlike existing RVAS  
35 tests, BATI allows integration of individual or variant-specific features as covariates, while  
36 efficiently performing inference based on full model estimation. We demonstrate that BATI  
37 outperforms established RVAS methods on realistic, semi-synthetic whole-exome sequencing  
38 cohorts, especially when using meaningful biological context, such as functional annotation. We  
39 show that BATI achieves power above 75% in scenarios in which competing tests fail to identify  
40 risk genes, e.g. when risk variants in sum explain less than 0.5% of phenotypic variance. We  
41 have integrated BATI, together with five existing RVAS tests in the 'Rare Variant Genome Wide  
42 Association Study' (rvGWAS) framework for data analyzed by whole-exome or whole genome  
43 sequencing. rvGWAS supports rare variant association for genes or any other biological unit  
44 such as promoters, while allowing the analysis of essential functionalities like quality control or  
45 filtering. Applying rvGWAS to a Chronic Lymphocytic Leukemia study we identified eight  
46 candidate predisposition genes, including EHMT2 and COPS7A.

## 47 Data availability and implementation

48 All relevant data are within the manuscript and pipeline implementation on  
49 <https://github.com/hanasusak/rvGWAS>

## 50 Author summary

51 Complex diseases are characterized by being related to genetic factors and environmental  
52 factors such as air pollution, diet etc. that together define the susceptibility of each individual to  
53 develop a given disease. Much effort has been applied to advance the knowledge of the genetic  
54 bases of such diseases, specially in the discovery of frequent genetic variants in the population  
55 increasing disease risk. However, these variants usually explain a little part of the etiology of  
56 such diseases. Previous studies have shown that rare variants, i.e. variants present in less than  
57 1% of the population, may explain the rest of the variability related to genetic aspects of the  
58 disease.

59 Genome sequencing offers the opportunity to discover rare variants, but powerful statistical  
60 methods are needed to discriminate those variants that induce susceptibility to the disease.  
61 Here we have developed a powerful and flexible statistical approach for the detection of rare  
62 variants associated with a disease and we have integrated it into a computer tool that is easy  
63 and intuitive for the researchers and clinicians to use. We have shown that our approach  
64 outperformed other common statistical methods specially in a situation where these variants  
65 explain just a small part of the disease. The discovery of these rare variants will contribute to the  
66 knowledge of the molecular mechanism of complex diseases.

## 67 Introduction

68 The rapidly improving yield and cost-effect ratio of Next Generation Sequencing (NGS)  
69 technologies provide the opportunity to study associations of genetic variants with complex  
70 multifactorial diseases in large cohorts at a genome-wide scale. As opposed to genome-wide  
71 association studies (GWAS), which are based on counting of genotypes at predefined genomic  
72 positions with alternative alleles of medium to high minor allele frequency in the population  
73 (MAF >1 %), whole-exome and whole-genome sequencing (WES, WGS) enable the study of

74 rare genetic variants (RV) across the whole exome or genome, respectively. Previous studies  
75 have shown that RVs play an important role in the etiology of complex genetic diseases(1–4).  
76 Furthermore, it has been demonstrated that RVs are more likely to affect the structure, stability  
77 or function of proteins than common variants(5,6). Therefore, statistical analysis of the  
78 combined set of rare variants across genes or regulatory elements has the potential to reveal  
79 new insights into the genetic heritability of complex diseases and the predisposition to cancer.  
80 To this end, rare variant association studies (RVAS) that facilitate identification of novel disease  
81 loci based on the burden of rare and damaging variants with low to medium effect size within  
82 genomic units of interest have been developed(7).  
83 One of the major difficulties when associating rare variants to disease is the lack of power when  
84 using traditional statistical methods like GWAS. Given that few individuals are carriers of the  
85 rare alternative allele, association studies based on single variant positions would require  
86 extremely large sample sizes. To overcome this obstacle and to increase statistical power,  
87 studies of RV consider simultaneously multiple variable positions within functional biological  
88 units, such as genes, promoters or pathways, for association to disease. Different statistical  
89 methods that address the problem of aggregated analysis of rare variants in case-control  
90 studies have been proposed. For example, score based methods pool minor alleles per unit into  
91 a measure of burden, which is used for association with a disease or phenotypic trait(8–11).  
92 These burden tests are powerful when a high proportion of RVs found in a gene affect its  
93 function and their effects on the disease are one-sided, i.e. either protective or deleterious. This  
94 is rarely the case since usually few deleterious variants coexist with many neutral and possibly  
95 some protective variants. Hence advanced methods have been developed to consider  
96 heterogeneous effects among RVs on the disease (or trait), which are mainly based on variance  
97 component tests, e.g. SKAT and C-alpha(12,13). These methods are more powerful than  
98 burden tests when the hypothesis of unidirectional effects does not hold(14). More recently,  
99 novel methods have been introduced. These contemplate that both types of genetic

100 architectures may coexist throughout the genome, by being constructed as a linear combination  
101 between burden and variance-component tests, such as SKAT-O(15). He et al.(16) developed  
102 an alternative method, a hierarchical Bayesian multiple regression model (HBMR) additionally  
103 accounting for variant detection errors commonly produced using NGS data, by incorporation of  
104 genotype misclassification probabilities in the model. Sun et al.(17) proposed a mixed effects  
105 test (MiST) within the framework of a hierarchical model, considering biological characteristics  
106 of the variants in the statistical model. In brief, MiST assumes that individual variants are  
107 independently distributed, with the mean modeled as a function of variant characteristics and  
108 certain variance that accounts for heterogeneous variant effects. In the resulting generalized  
109 linear mixed effects model (GLMM) variant-specific effects are treated as the random part of the  
110 model and patient and variant characteristics as the fixed part. The authors claim that, under the  
111 assumption that associated variants share common characteristics such as similar impact on  
112 protein function (e.g. primarily loss of function), using this prior information increases the power  
113 of the test. However, they also note that attempting to estimate the full model for inference  
114 purposes requires multiple integration, such that it becomes too computationally intensive for a  
115 genome-wide scan. Instead, a score test under the null hypothesis of no association is  
116 proposed, avoiding multiple integration.

117 Building on the concept of MiST, but with the motivation of making inference based on full  
118 model estimation, we propose a Bayesian alternative to the GLMM, using the Integrated Nested  
119 Laplace Approximation (INLA) for efficient model estimation(18). Calculating the marginal  
120 likelihood to estimate complex models in a fully Bayesian manner is often infeasible. Therefore,  
121 approximate procedures such as the heuristic Markov Chain Monte Carlo (MCMC) method are  
122 conventionally applied(16). MCMC is a highly flexible approach that can be used to make  
123 inference for any Bayesian model. However, evaluating the convergence of MCMC sampling  
124 chains is not straightforward(19). Another concern with MCMC is the extensive computation  
125 time, especially in large-scale analyses such as genome-wide scans. INLA is a non-sampling

126 based numerical approximation procedure, developed to estimate hierarchical latent Gaussian  
127 Markov random field models. Being based on numerical approaches instead of simulations  
128 renders INLA substantially faster than MCMC. Furthermore, Rue and Martino(20) demonstrated  
129 for several models that INLA is also more accurate than MCMC when given the same  
130 computational resources. The flexibility of modeling within the Bayesian framework combined  
131 with rapid inference approaches opens new possibilities for genetic association testing.  
132 Here, we present a novel Bayesian rare variant Association Test using INLA (BATI),  
133 implemented as part of the ‘Rare Variant Genome Wide Association Study’ (rvGWAS)  
134 framework. rvGWAS combines quality control (QC), interactive filtering, detection of data  
135 stratification (technical or population based), integration of functional variant annotations and  
136 four commonly used rare variant association tests (Burden, SKAT-O, KBAC and MiST) as well  
137 as the two Bayesian alternatives, HBMR and BATI. We demonstrate using realistic benchmarks  
138 that BATI substantially outperforms existing methods if prior information on the effect of variants  
139 on protein function is used. We further show that BATI successfully copes with complex  
140 population structure and other confounders. Finally, we propose how to use ‘difference in  
141 deviance information criterion’ ( $\Delta$ DIC) for model selection.

## 142 Material and Methods

### 143 **Bayesian rare variant Association Test based on Integrated nested Laplace 144 approximation (BATI).**

145 Integrated Nested Laplace Approximation is a recent approach to implement Bayesian inference  
146 on latent Gaussian models, which are a versatile and flexible class of models ranging from  
147 (generalized) linear mixed models (GLMMs) to spatial and spatio-temporal models. A detailed  
148 definition of INLA can be found in(18,21,22). Here we applied INLA using the implementation of

149 the R-INLA project (R package INLA version 17.06.20) to build a hierarchical Bayesian  
150 approach to the GLMM for the association of rare variants with phenotypes in the context of  
151 case-control studies. Our method termed BATI can efficiently and flexibly integrate a large  
152 number of categorical and numeric characteristics of genetic variants as covariates, as INLA  
153 facilitates estimation of the full model even for complex structures of random effects.

154 **Model specification**

155 Assume we have  $N$  individuals, and let  $Y_i$  ( $i = 1, \dots, N$ ) be the observed phenotype of the  $i^{\text{th}}$   
156 individual that belongs to an exponential family:

157 
$$Y_i \sim \pi(Y_i; \mu_i, \theta) \quad (1)$$

158 where the expected value  $\mu = E(Y_i)$  is linked to a linear predictor  $\eta_i$  through a known link  
159 function  $g(\cdot)$ , so that  $g(\cdot) = \eta_i$ . In our case  $Y_i$  is a binary variable representing affected  
160 individuals (cases) vs. unaffected individuals (controls). We propose to construct the likelihood  
161 of the data based on a logistic distribution and use the identity function for  $g(\cdot)$ . The linear  
162 predictor  $\eta_i$  is defined to account for potential confounding covariates at the individual level as  
163 well as for covariates at the variant level such as a variant's functional impact:

164 
$$\eta_i = X_i^t \alpha + G_i^t \beta \quad (2)$$

165 where  $X_i$  is a  $m \times 1$  vector of individual-based confounding covariates and  $G_i$  denotes a  $p \times 1$   
166 vector of genotypes for  $p$  RVs. Each genotype is coded as 0, 1, or 2, representing the number of  
167 minor alleles.  $\alpha$  and  $\beta$  are the regression vectors of coefficients.

168 BATI can account for individual variant characteristics under the assumption that similar variant-  
169 specific characteristics have a similar effect on the function of the protein and hence the  
170 phenotype, while still allowing for potential variant-specific heterogeneity effects. Thus  $\beta$  can be  
171 modeled in a hierarchical way as:

172 
$$\beta_j = Z_j^t \omega + \delta_j \quad (3)$$

173 where  $\omega$  is a vector of  $q \times 1$  ( $j = 1, \dots, q$ ) variant-specific regression coefficients,  $Z^t$  is a  $p \times q$   
174 matrix (for  $q$  covariates per variant), and  $\delta$  is a  $p \times 1$  random effects vector which is assumed to  
175 follow a multivariate Gaussian distribution with mean 0 and covariance matrix  $\tau Q$ . If no  
176 dependency structure is defined across variants, as in MiST(17),  $Q$  is a  $p \times p$  identity matrix and  
177  $\tau$  the random effects variance. However, in order to model a correlation structure between  
178 variants, such as physical distance dependency, BATI allows to construct  $Q$  such that it reflects  
179 this structure. This is enabled by INLA, which provides Laplace approximation of the posterior  
180 distributions, therefore allowing the estimation of the full model for complex structures of random  
181 effects.

182 Plugging equation (3) into (2) we obtain the expression of a generalized linear mixed effects  
183 model (GLMM):

184 
$$\eta_i = X_i^t \alpha + (G_i^t Z) \omega + G_i^t \delta \quad (4)$$

185 with  $\alpha$  and  $\omega$  as fixed effects coefficients and  $\delta$  as random effects coefficients. Given the vector  
186 of parameters  $\theta = \{\alpha, \omega, \delta\}$ , the objectives of the Bayesian computation are the marginal posterior  
187 distributions for each of the elements of the parameter vector  $p(\theta_s | y)$  and for the hyper-  
188 parameter  $p(\tau | y)$ . In order to compute the marginal posterior for the parameters, we first need  
189 to compute  $p(\tau | y)$  and  $p(\theta_s | \tau, y)$ . The INLA approach exploits the assumptions of the model to  
190 produce a numerical approximation to the posteriors of interest, based on the Laplace  
191 approximation(23).

192 **Model selection**

193 The classical approaches of association tests are based on hypothesis testing, where the null  
194 hypothesis assumes no genetic effects, and the alternative hypothesis assumes a genetic effect  
195 on the phenotype. In the context of BATI this can be specified as follows:

196 
$$H_0: \eta_i = X_i^t \alpha \quad (5)$$

197 
$$H_1: \eta_i = X_i^t \alpha + (G_i^t Z) \omega + G_i^t \delta \quad (6)$$

198 A classic Bayesian criterion for model goodness of fit is the *Deviance Information Criteria (DIC)*  
199 )(24). *DIC* is calculated as the expectation of the deviance over the posterior distribution plus the  
200 effective number of parameters. Thus, difference in *DIC* between the  $H_0$  and the  $H_1$  models,  
201  $\Delta DIC = DIC_{H_0} - DIC_{H_1}$ , can be used as the model selection criteria. As a rule of thumb values of  
202  $\Delta DIC > 10$  are recommended to reject the null-hypothesis. However, to evaluate the ability of  
203  $\Delta DIC$  to correctly choose between null or alternative models we suggest the use of simulations,  
204 as proposed by Holand et al.(25). To find an estimate of the probability of type I error,  
205 concluding that there are genetic effects when in truth there is none, we randomly assign  
206 individuals to either cases or controls. We then adjust models under null and alternative  
207 hypothesis for each gene or biological unit included in the genome wide study, obtaining the  
208 empirical distribution of  $\Delta DIC$ . Finally, we select a  $\Delta DIC$  threshold from the quantile  
209 corresponding to the desired significance level. For more robust threshold estimation, we  
210 propose to generate  $S$  datasets by randomly shuffling cases and controls, such that  $S$   $\Delta DIC$   
211 thresholds can be obtained and the median of the thresholds can be used. We used  $S = 10$  for  
212 model selection in our benchmark study.

213

#### 214 **A comprehensive framework for rare variant association analysis (RVAS).**

215 We developed the ‘Rare Variant Genome Wide Association Study’ (rvGWAS) framework (Fig  
216 1A and Supplementary S1 Fig), an all-in-one tool designed for RVAS tests using case-control  
217 cohorts analyzed by NGS. rvGWAS supports rare variant association aggregating by genes or  
218 any other biological unit such as promoters or enhancers. It provides all essential steps and  
219 functionalities to perform the complete analysis of whole-exome sequencing (WES) or whole-  
220 genome sequencing (WGS) based case-control study designs: (1) it facilitates comprehensive  
221 quality control and filtering, (2) it evaluates data stratification (either technical or population  
222 based), (3) it enables the integration of patient- and/or variant-based covariates in association

223 tests in an easy and intuitive fashion, and (4) it integrates six conceptually different rare-variant  
224 association methods. It is implemented in a modular way and provides great flexibility, allowing  
225 to analyze a wide range of association study designs.

226

227 **Fig 1. rvGWAS workflow and QC plots for 1810 high quality samples from 1000GP used**  
228 **for benchmarking.** (A) rvGWAS workflow for performing QC and six RVAS tests. The QC  
229 module computes quality statistics shown in panels B-F. The result of each RVAS test is a  
230 ranked list of genes with various informative attributes. (B) Bar-plot for number of variants per  
231 sample, colored by functional annotation of variants. (C) Barplot for number of variants per  
232 sample, colored by assignment to cases (~1/2) or controls (~1/2). (D) Number of variants per  
233 gene in cases (x-axis) and controls (y-axis). Each dot is one gene, while the red line shows the  
234 ratio of the number of cases and controls (1:1). (E) Histogram for number of mutations per  
235 sample after removal of outliers. (F) Projection on first 10 PCA components. Samples are  
236 colored by sequencing center. The graph in the upper right corner shows the cumulative  
237 percentage of variance explained per principal components. Principal components can be used  
238 as covariates in several RVAS tests.

239

240 BATI and five other RVAS methods are integrated in the rvGWAS framework. KBAC, SKAT-O,  
241 and MiST, were chosen to be included due to their superior performance compared to eight  
242 other RVAS methods in a benchmark study by Moutsianas et al.(14). In addition, we included  
243 the classical Burden test representing the most simplistic and intuitive form of RVAS tests.  
244 Finally, we incorporated HBMR, which is conceptually the most similar to BATI in terms of its  
245 estimation approach (while MiST is more similar in terms of model specification). The six  
246 supported RVAS tests represent a broad spectrum of approaches, including classic aggregation  
247 of variants as a Burden variable, variance component bidirectional tests, mixed effect models  
248 and Bayesian inference.

249 rvGWAS is implemented as a pipeline of R scripts, and is available online at  
250 <https://github.com/hanasusak/rvGWAS>. Detailed descriptions of the tool, included methods as  
251 well as parameters are provided in supporting information file.

252

253 **Realistic ‘semi-synthetic’ simulations of whole-exome sequencing based case-control  
254 studies.**

255 To allow for benchmarking using highly realistic disease cohorts, which correctly represent all  
256 expected sources of noise, we developed a new disease cohort simulator combining thousands  
257 of real WES datasets from various studies with known risk variants for a selected disease type.  
258 The simulator randomly assigns WES samples to the case or control group and introduces  
259 predisposition variants found in ClinVar for a disease of choice into the VCF files of cases.

260 We used two large datasets as basis for the simulation: 1) WES data of the 1000 Genomes  
261 Project (1000GP), and 2) an in-house dataset combining patients diagnosed with various  
262 conditions and healthy individuals subjected to WES during 2012 to 2017. VCF files from

263 1000GP (phase3)(26,27) were downloaded from  
264 <ftp://ftp.1000genomes.ebi.ac.uk/vol1/ftp/release/20130502/>. This cohort contains 2504  
265 individuals from 26 populations. WES libraries of 1000GP were prepared using one of four oligo  
266 enrichment kits: (1) Nimblegen SeqEz V2, (2) Nimblegen SeqEz V3, (3) VC Rome, and (4)  
267 Agilent SureSelect V2. Additional sample information used as covariates (population, super  
268 population, gender) was obtained from the file  
269 integrated\_call\_samples\_v3.20130502.ALL.panel. We excluded related individuals, e.g. in  
270 parent-child trios we included the parents (if not consanguineous), but not the child. To minimize  
271 issues with population stratification due to highly diverse populations we only included  
272 individuals not belonging to African ancestry populations, as Africans had on average 25% more  
273 variants than individuals from other ancestry groups. Nonetheless, the remaining cohort still

274 represents a mixed population, allowing us to benchmark population stratification efficiency of  
275 the RVAS tests.

276 The in-house 'Iberian' WES cohort includes 1189 individuals of Spanish ancestry and is  
277 therefore highly homogeneous. WES libraries were prepared using three different oligo  
278 enrichment kits: (1) Agilent SureSelect 50, (2) Agilent SureSelect 71, and (3) Nimblegen SeqEz  
279 V3. Computational analysis and variant calling was performed according to GATK best practice  
280 guidelines (<https://software.broadinstitute.org/gatk/best-practices/>). For simulation purposes we  
281 only considered genomic loci that were targeted and covered with at least 10 sequence reads  
282 by all oligo enrichment kits, and variants with a call rate higher than 85%. Samples that were  
283 identified as outliers based on the number of called variants, transition to transversion (Ti/Tv)  
284 ratio, or their projection on the first two principal components from principal component analysis  
285 were removed from further analysis. The remaining datasets, named 1000GP and Iberian  
286 cohort, consisted of 1,810 and 1,167 samples harboring 493,314 and 285,658 unique loci with  
287 alternative alleles, respectively. From 1000GP we randomly selected half of the samples as  
288 cases, the other half as controls, while for the Iberian cohort we selected one third as cases,  
289 and two thirds as controls.

290

### 291 **Simulating a breast cancer risk cohort.**

292 To introduce realistic disease variants into a 'semi-synthetic' breast cancer predisposition  
293 cohort, we queried the ClinVar database for breast cancer risk variants annotated as exonic or  
294 splicing. We removed variants that had MAF higher than 0.01 in any ancestry population in any  
295 of three commonly used exome databases: EVS, 1000GP or ExAC. Six genes had more than  
296 five annotated disease risk variants in ClinVar: *BRCA2* (MIM: \*600185), *BRCA1* (MIM:  
297 \*113705), *PALB2* (MIM: \*610355), *BRIP1* (MIM: \*605882), *CHEK2* (MIM: +604373) and *BARD1*  
298 (MIM: \*601593) (Supplementary S1 Table), which we used to simulate risk patients by adding  
299 variants to the VCF files (zero or one variant per case). As expected, all six genes already had

300 rare variants, likely benign, in the unmodified cohorts (Supplementary S2 Table and  
301 Supplementary S3 Table). This type of noise is expected in any case-control study using WES  
302 data, and hence makes the simulation more realistic. We generated three genetic architectures  
303 per gene, with ~2% (1), ~1% (2) or ~0.5% (3) of phenotypic variance explained (VE) by  
304 introducing ClinVar risk variants. To this end we used the method of So et al.(28) for calculation  
305 of cumulative VE each time a variant was added to a gene until the targeted VE was reached.  
306 Calculation of VE requires three parameters per each variant: the prevalence of the trait, the  
307 population frequency of the risk allele, and the genotype relative risk (RR). In practice, only odds  
308 ratios (OR) are available in many case-control studies. However, OR approximates RR when  
309 the disease prevalence in a population is low(28). As prevalence of breast cancer we selected  
310 an estimate for the Spanish population of 0.00085(29). In order to generate realistic RR  
311 distributions, we generated a distribution (Supplementary S2 Fig) assuming that the likelihood of  
312 having high RR is negatively correlated with MAF(14). For *BRCA1* and *BRCA2* we simulated  
313 two different types of genetic architectures, by introducing in one architecture only missense  
314 variants, and in the other only loss of function (LoF) SNVs (i.e. stop-gain, stop-loss or splicing).  
315 This allowed us to test if MiST and BATI benefit from features that capture biological function  
316 and context of variants. For the four remaining genes, the variants were simulated regardless of  
317 their functionality. The simulation procedure is repeated 100 times for each of the 8  
318 architectures in order to generate 100 datasets for evaluation of statistical power and type I  
319 error rates (TIER). For *BARD1* it was not possible to reach the desired VE of 2% and 1% in  
320 most simulations due to an insufficient number of breast cancer risk variants found in ClinVar.  
321 Supplementary S3 Fig and Supplementary S4 Fig show the exact levels of VE in 100  
322 simulations per gene for each of the two cohorts.

## 323 Results

### 324 **Quality control and filtering of benchmark WES cohorts.**

325 Cohorts used for benchmarking of test methods consisted of 1,810 individuals in the 1000GP  
326 cohort and 1,167 individuals in the Iberian cohort, harboring 493,314 and 285,658 unique loci  
327 with a non-reference genotype in at least one of the samples, respectively. Both datasets were  
328 analyzed and filtered using the rvGWAS quality control modules (see Methods and Supporting  
329 information file). For benchmarking purposes, we only considered variants in regions targeted  
330 by all used oligo enrichment kits. However, in the case of the Iberian cohort we observed that a  
331 small subset of regions supposed to be targeted consistently showed low coverage in a kit-  
332 specific manner, leading to strong biases identified by the data stratification module of rvGWAS  
333 (data not shown). The bias disappeared when excluding regions with less than 10x average  
334 coverage in at least one kit (Supplementary S5F Fig). Samples included in the final simulation  
335 cohorts show no biases in any of the first ten components of the PCA (1000GP: Fig 1F, Iberian:  
336 Supplementary S5F Fig), and the explained variance per PCA component is low (Fig 1F,  
337 Supplementary S5C Fig). Furthermore, samples in the two cohorts show a normal distribution of  
338 the number of mutations (Fig 1E, Supplementary S5E Fig) and Ti/Tv ratio (data not shown), and  
339 show no bias in the number of variants and fractions of InDels or synonymous, nonsynonymous  
340 and LoF SNVs (Fig 1B, Fig 1C, Supplementary S5A-B Fig). Finally, there is a high correlation  
341 between the fraction of cases and of controls having variants in any given gene (Fig 1D,  
342 Supplementary S5D Fig).

343

### 344 **Benchmarking RVAS Tests using semi-synthetic breast cancer risk cohorts.**

345 We used the rvGWAS framework to benchmark the six RVAS tests (Burden, SKAT-O, KBAC,  
346 MiST, HBMR and BATI) on the 1000GP and Iberian cohorts with simulated breast cancer risk  
347 variants. In order to simulate a realistic breast cancer predisposition case-control study we

348 randomly split each of the original cohorts in a case (1000GP: 905, Iberian: 389 samples) and a  
349 control group (1000GP: 905, Iberian: 778 samples), and, in the case group samples, added  
350 ClinVar risk variants to the genes *BRCA2*, *BRCA1*, *PALB2*, *BRIP1*, *CHEK2* and *BARD1* using  
351 realistic variance explained (VE) rates (see Methods). Before performing the RVAS we filtered  
352 out common variants (AF>0.01 in public databases or in the randomized control group) as well  
353 as variants that were annotated as synonymous or had a CADD score below 10 (likely benign,  
354 see <https://cadd.gs.washington.edu/info>). For BATI and MiST we used prior information on  
355 variant characteristics as covariates: CADD scores as a quantitative variable and exonic  
356 function (missense, loss-of-function, InDels) as a categorical variable. We repeated the  
357 simulation and benchmarking process 10 times, including the randomized case-control  
358 assignment in order to randomize background noise in each benchmark cycle.

359 **Type I Error Rate estimates.**

360 The six benchmarked RVAS tests use diverse criteria for statistical significance (p-value, Bayes  
361 factor or  $\Delta DIC$ ). To generate comparable significance thresholds, we performed RVAS tests on  
362 randomly split cohorts, but without introduced ClinVar risk variants. Hence, significant  
363 associations should only be found by random chance and constitute false positives. This  
364 procedure allowed us to obtain comparable thresholds for desired type I error rates for all  
365 methods. For each of the 10 random cohort splits we obtained p-value significance thresholds  
366 for Burden, KBAC, SKAT-O and MiST that translate to 5%, 0.1% and 0.01% TIER. Similarly, for  
367 HBMR and for BATI we calculated thresholds for Bayes factor and  $\Delta DIC$  resulting in the same  
368 TIER levels. Estimated thresholds are highly similar across all 10 randomized case-control splits  
369 (Supplementary S6 Fig). At 0.01% TIER only 2 genes (out of ~20,000) are expected as  
370 significant by chance, therefore the observed small fluctuation of estimated significance  
371 thresholds is not surprising. We finally used the test-specific median from 10 random splits as  
372 thresholds to label a gene as significant for subsequent power analyses (Supplementary S6  
373 Fig, Table 1 and Supplementary S4 Table).

374

375 **Table 1 P-value, Bayes Factor (HBMR) and  $\Delta$ DIC (BATI) thresholds for Type I error rates**  
376 **(TIER) of 0.05, 0.001 and 1e-04 estimated on 1000GP.** We randomly permuted case and  
377 control labels 10 times and for each estimated empirical thresholds for each RVAS test. The  
378 median TIER values from 10 random permutations are used as thresholds for benchmark  
379 comparison.

Method	0.05 TIER	0.001 TIER	1e-04 TIER
BURDEN	0.0519	1.12e-03	7.79e-05
KBAC	0.0650	1.52e-03	1.52e-04
SKAT-O	0.0563	1.47e-03	1.66e-04
MiST	0.0766	2.26e-09	3.33e-16
HBMR	1.2678	3.5774	9.0838
BATI	2.3898	9.5929	14.4623

380

381

382 We noticed that MiST shows zero inflated p-values (Supplementary S7A Fig). These  
383 unexpected zero p-values occur exclusively for genes with few variants (<10) across the cohort,  
384 indicating that the MiST method fails to obtain accurate p-values for genes with low burden of  
385 variants. Hence, we removed all genes with p-value 0 from MiST results (Supplementary S7B  
386 Fig). No other method showed a p-value inflation artefact or unexpectedly high Bayes Factor or  
387  $\Delta$ DIC values (Supplementary S7C-G Fig).

388

389 **Power analysis for six RVAS test methods.**

390 We next determined the power of the competing RVAS tests to identify the 8 breast cancer risk  
391 genes (*BRCA1-Missense*, *BRCA1-LoF*, *BRCA2-Missense*, *BRCA2-LoF*, *PALB2*, *BRIP1*,  
392 *CHEK2* and *BARD1*) at the three TIER levels 5%, 0.1% and 0.01% and at three levels of VE of

393 2%, 1% and 0.5% (1000GP: Fig 2, Iberian: Supplementary S8 Fig). For the 1000GP cohort we  
394 found that all methods showed a power close to 100% at a TIER of 5% across all tested VE  
395 levels, except for Burden and KBAC, which showed decreased performance for VE = 0.5% (Fig  
396 2A-C left). Testing 20,000 genes (whole exome) at a TIER of 5% we expect around 1000 false  
397 positive genes, which is a poor choice for most studies. Using a TIER of 0.1% (~20 false  
398 positive genes expected), differences between the tests become more pronounced, with  
399 Burden, KBAC and MiST showing decreased power already for 1% VE, and all methods except  
400 for BATI showing decreased power at 0.5% VE (Fig 2A-C middle). Interestingly, Burden, KBAC  
401 and SKAT-O show strongly fluctuating power for the 8 tested genes, often showing either 100%  
402 or 0% power (Fig 2C middle), meaning a risk gene was either identified in all 100 simulations, or  
403 in none. BATI achieved more than 75% power for all genes, with a median above 90%. Using a  
404 strict TIER of 0.01% (2 false positives expected for the whole exome), all tools except for MiST  
405 are able to identify risk genes at 2% VE at almost 100% (for the outlier *BARD1* we did not  
406 achieve 2% VE in all simulations due to a lack of variants in ClinVar). However, performance of  
407 all methods except BATI drops substantially for 1% VE. At 0.5% VE most methods miss the  
408 majority of risk genes in the majority of simulations (median power close to zero), while BATI  
409 still achieves a median power of 60% (Fig 2A-C right). Note that MiST performed very poorly for  
410 the strict TIER thresholds of 0.1% and 0.01%, likely due to the aforementioned zero-p-value  
411 inflation issue, which results in a large number of false positives.

412

413 **Fig 2. Benchmarking power of RVAS methods for the 1000GP-based BRCA risk study.**  
414 *Each dot in the plots represents one of simulated 8 risk genes, and y-axis values show the  
415 fraction of 100 simulations in which the gene was called as significant. RVAS tests were  
416 benchmarked under the following 9 settings. Variance explained (VE) of the incorporated risk  
417 variants is (A) ~2%, (B) ~1%, and (C) ~0.5%. For each VE we tested three TIER levels, left:  
418 TIER 5%, middle: TIER 0.1%, and right: TIER 0.01%.*

419

420 Results are mostly similar in the benchmark using the Iberian cohort (Supplementary S8 Fig).  
421 However, most tests perform slightly worse due to the smaller size of the cohort (1,167 vs  
422 1,810 total individuals). Notably, BATI's performance is stable despite the smaller cohort size.  
423 Specifically, for a low VE of 0.5% and a strict TIER of 0.01% (Supplementary S8 Fig right), all  
424 methods except for BATI show power close to 0, while BATI achieves power close to 100% for  
425 three risk genes (median power of 55%).

426

#### 427 **Risk gene-wise power analysis.**

428 Each gene has a different architecture, i.e. rate of (likely benign) rare variants in the original  
429 cohorts, functional impact estimates for known risk variants, fraction of stop-gain or splicing  
430 variants etc. We therefore benchmarked the performance of all RVAS tests across 100  
431 simulations of risk variants for each gene separately (1000GP cohort: Fig 3 and Table 2,  
432 Iberian cohort: Supplementary S9 Fig). In the gene-wise power plots we indicate the three TIER  
433 thresholds using red (5%), green (0.1%) and blue (0.01%) lines. Note that due to different y-Axis  
434 scaling these lines are not on the same height for different tests. As expected all methods  
435 except MiST identify all risk genes at 0.01% TIER in the 2% VE setting. However, substantial  
436 differences in power of the tests appear when VE is only 1% or 0.5%. While BATI calls most  
437 genes with TIER 0.01% even at VE of 0.5%, and all genes at TIER 0.1% with >80% power  
438 (Table 2), Burden, KBAC and SKAT-O recurrently fail to call *BRCA2* (both missense and LoF  
439 versions), and HBMR fails to call *BARD1*, *CHEK2* and *PALB2* already at TIER 0.1% (Table 2).  
440 The performance of Burden, KBAC and SKAT-O varies considerably between genes, while  
441 MiST, HBMR and BATI show relatively small differences. Interestingly, the power plots at 0.5%  
442 VE look very similar when comparing Burden, KBAC and SKAT-O, indicating that these  
443 methods share the same strengths and weaknesses.

444

445 **Fig 3. Benchmarking statistical power to detect rare variant associations for 8 genes**  
 446 *individually*. Rare variants annotated for increased breast cancer risk were simulated into the  
 447 1000GP dataset with cases and controls randomly assigned. Power (y-axis) per gene for 6  
 448 methods (Burden, KBAC, SKAT-O, MiST, HBMR and BATI) is shown for (A) 2%, (B) 1%, and  
 449 (C) 0.5% variance explained between cases and healthy controls. (Due to using real SNVs in  
 450 the simulation the variance explained per gene fluctuates slightly around the targeted VE. See  
 451 Supplementary S3 Fig). Lower, middle and upper lines indicate relaxed (5%), medium (0.1%)  
 452 and strict (0.01%) TIER thresholds, respectively.

453

454 **Table 2 Power of six RVAS methods for 8 genes/architectures simulated using the**  
 455 **1000GP cohort and ClinVar disease variants**. 100 Architectures were simulated for each  
 456 gene. For BRCA1 and BRCA1 simulation was performed in missense and in LoF mode (see  
 457 Methods). Power is shown for VE = 0.05% and TIER levels 0.001 and 1e-04.

Gene Method	BRCA1 MiSS	BRCA1 LoF	BRCA2 MiSS	BRCA2 LoF	BARD1	BRIP1	CHEK2	PALB2
BURDEN	99	<b>100</b>	0	0	0	<b>100</b>	13	54
KBAC	<b>100</b>	<b>100</b>	0	0	5	<b>100</b>	30	68
SKAT-O	99	<b>100</b>	0	0	0	<b>100</b>	10	78
MiST	0	0	0	0	0	0	0	0
HBMR	78	78	87	82	2	98	26	1
BATI	98	<b>100</b>	<b>88</b>	<b>99</b>	<b>79</b>	98	<b>77</b>	<b>93</b>
BURDEN	57	60	0	0	0	58	1	5
KBAC	<b>86</b>	92	0	0	0	<b>100</b>	4	13
SKAT-O	79	86	0	0	0	<b>100</b>	1	15
MiST	0	0	0	0	0	0	0	0
HBMR	0	0	0	0	0	0	2	0
BATI	63	<b>94</b>	<b>56</b>	<b>74</b>	<b>9</b>	68	<b>29</b>	<b>57</b>

458

459 Only MiST and BATI are able to leverage categorical variant characteristics, here represented  
460 as functional annotations such as ‘missense’, ‘LoF’, ‘indel’. As background LoF variants are rare  
461 we expected that both methods excel at predicting *BRCA1* and *BRCA2* under the LoF-  
462 architecture simulation. Indeed, for both methods we see a better performance for *BRCA1*-LoF  
463 and *BRCA2*-LoF compared to the *BRCA1*-missense and *BRCA2*-missense, respectively. For  
464 BATI, this difference is significant for both genes (*BRCA1*:  $p = 4.0\text{e-}13$  and *BRCA2*:  $p = 0.0025$   
465 for  $\text{VE} = 0.5$  using Wilcoxon rank test). As a result, BATI predicts *BRCA2*-LoF at the highest  
466 significance level (TIER 0.01%), while all other methods perform poorly. *BRCA1*-LoF shows the  
467 highest  $\Delta\text{DIC}$  value from all 8 risk genes, demonstrating that the BATI method strongly benefits  
468 from categorical functional annotations.

469 The strong performance of BATI in terms of precision and recall comes at the price of longer run  
470 time (Supplementary S5 Table). Inference based on full model estimation leads to a higher  
471 computational complexity and hence higher run time of BATI compared to all competing  
472 methods. The computational time and complexity of RVAS test methods is a concern, as exome  
473 and genome sequencing datasets have been increasing dramatically in sample size recently.  
474 However, the INLA implementation used by BATI (R-INLA project) facilitates the use of multiple  
475 cores, and scales close to linearly with the number of used cores, allowing for analysis of large  
476 cohorts on modern servers with many cores. Moreover, lowering the allele frequency threshold  
477 of included rare variants (e.g. from  $\text{AF} \leq 1\%$  to  $\text{AF} \leq 0.1\%$ ) for very large cohorts can  
478 dramatically reduce computation times.

479

#### 480 **RVAS of chronic lymphocytic leukemia identifies candidate risk genes.**

481 Chronic lymphocytic leukemia (CLL) is a cancer of B-lymphocytes, which expands in the bone  
482 marrow, lymph nodes, spleen and blood. With the aim to identify the landscape of germline risk  
483 genes that can predispose an individual to CLL, we applied BATI and the other five competing

484 RVAS methods integrated in rvGWAS. The CLL cohort of 436 cases was collected and  
485 sequenced following the guidelines of the International Cancer Genome Consortium (ICGC)(30)  
486 within the framework of the Spanish ICGC-CLL consortium(31) (Puente *et al.* 2015). In addition,  
487 725 individuals from our Iberian cohort were used as controls. For the gene-wise RVAS test we  
488 preselected rare (MAF≤ 0.01 in our control cohort, ExAC and 1000GP) and potentially  
489 damaging variants (CADD score > 10). All RVAS methods were adjusted for the first 10  
490 principal components to account for population stratification and technical biases. For BATI and  
491 MiST we additionally added the exonic function of the variants (i.e. LoF, missense, indel) and  
492 the CADD damage score as covariates. We tested all genes with a variant call rate of at least  
493 95% and removed genes flagged by Allele Balance Bias (ABB)(32) as enriched with false  
494 positive variant calls (see Supporting information file for details). BATI identified 12 candidates  
495 that passed the significance threshold of 10<sup>-4</sup> (Supplementary S6 Table). Among those, EHMT2  
496 and COPS7A are promising CLL risk gene candidates. The heterodimeric methyltransferases  
497 EHMT1 and EHMT2 have recently been implicated with prognosis of CLL and CLL cell  
498 viability(33). COPS7A (previous name COP9) is involved in the Transcription-Coupled  
499 Nucleotide Excision Repair (TC-NER) pathway and the COP9 signalosome complex (CSN) is  
500 involved in phosphorylation of p53/TP53, JUN, I-kappa-B-alpha/NFKBIA, ITPK1 and  
501 IRF8/ICSBP. However, replication of results in independent cohorts is required to evaluate  
502 these findings.

## 503 Discussion

504 Here we presented a comprehensive framework, rvGWAS, to facilitate user-friendly and intuitive  
505 analysis of RVAS in case-control studies using whole genome or custom-captured next  
506 generation sequencing data. rvGWAS integrates data quality control and filtering, several  
507 existing rare variant association tests and the newly developed BATI test. We showed how BATI

508 leverages both categorical and numerical variant characteristics and strongly benefits from their  
509 inclusion as covariates. We demonstrated BATI's significant gain in power if risk genes contain  
510 mostly LoF variants, while still performing at least as good as other methods when testing genes  
511 containing mostly missense variants.

512 Model estimation when using complex data structures, including exome-wide genetic variants,  
513 numerical damage estimates and functional annotations, becomes computationally heavy.  
514 Therefore, existing tests do not estimate the full model (as in MiST) or use the relatively slow  
515 MCMC (as in HBMR). BATI addresses this issue by estimating the full model using Integrated  
516 Nested Laplace Approximation, which requires reasonable computational resources even when  
517 using complex data structures. INLA provides approximations to the posterior marginals of the  
518 latent variables, which are accurate and extremely fast to compute(18). INLA was originally  
519 developed as a computationally efficient alternative to MCMC and presents two major  
520 advantages. On the one hand, INLA's fast speed allows it to work on models with huge  
521 dimensional latent fields and a large number of covariates at different hierarchical levels (for  
522 example in case of RVAS at the patient level and at the variant level). On the other hand, INLA  
523 treats latent Gaussian models in a unified way, thus allowing for greater automation of the  
524 inference process. Thanks to these characteristics, INLA has already been used in a great  
525 variety of applications(34–39). Leveraging the efficiency of INLA, BATI, unlike MiST, can make  
526 inference based on full model estimation, and provides comprehensive information on estimates  
527 of model parameters. Furthermore, BATI allows for the inclusion of many numerical or  
528 categorical features as covariates. Which other features, in addition to functional impact and  
529 functional annotation of variants, could be beneficial for association testing remains to be  
530 determined. Promising categories include variant call quality, tissue-specific gene expression  
531 measures, biological pathways or copy number variants.

532 Previous benchmark studies of RVAS tests typically relied on pure simulations of variants, for  
533 instance based on HapMap statistics, resulting in completely artificial cohorts(14). Furthermore,

534 simulations were often restricted to small regions of the genome, limiting their power for  
535 benchmarking exome-wide association tests. Simulated variant data is well-known to lack the  
536 complexity and noise-level of real data, resulting in overly optimistic benchmark performances  
537 and unrealistic expectations of the clinical researchers. Moreover, the use of random ‘causal’  
538 variants hampers the benchmarking of methods that leverage characteristics of causal disease  
539 variants, which are enriched in high damage scores and high impact changes such as LoF  
540 variants. Here we combined real WES cohorts, representing realistic background noise, with  
541 real disease variants, featuring realistic functional impact profiles and variant distributions, to  
542 form semi-synthetic benchmark cohorts. We developed sampling methods allowing to test  
543 different disease architectures featuring various levels of variance explained in multiple risk  
544 genes. Furthermore, tests in the original randomized cohorts without introduced disease  
545 variants facilitated the translation of method-specific significance thresholds to comparable  
546 thresholds for type I error rates.

547 Using these simulations, we show that methods vary substantially in power, especially for risk  
548 genes explaining a small fraction of the variance in a cohort. We found that differences between  
549 methods when VE is low (1% and 0.5%) are substantially more profound than previously  
550 appreciated, with some methods showing strongly fluctuating success rates for different genes  
551 and close to zero power at VE of 0.5%. For example, MiST showed favorable results on purely  
552 artificial benchmark sets(14), but performed poorly on our realistic WES cohorts, likely due to an  
553 issue with zero-inflated p-values caused by inappropriate handling of low variant counts.  
554 Specifically, MiST failed to identify any risk gene at low VE or low TIER thresholds. We further  
555 found that the performance patterns of Burden, KBAC and SKAT-O across the 8 risk gene  
556 architectures are highly similar when compared to MiST, HBMR and BATI. Burden, KBAC and  
557 SKAT-O fail to predict the same genes at 0.5% VE, namely BRCA2, BARD1 and CHEK2, which  
558 are characterized by high numbers of benign background variants. It is therefore likely beneficial

559 to combine Burden- and SKAT-type methods with completely different approaches to  
560 compensate for Burden and SKAT specific weaknesses.

561 In summary, leveraging variant characteristics and using the fast and accurate INLA model  
562 estimation, BATI outperforms existing RVAS test methods on realistic WES cohorts using real  
563 disease variants in 8 breast cancer risk genes, in hundreds of permutations. By facilitating  
564 integration of large numbers of covariates, BATI represents a flexible testing approach that can  
565 be further extended and enhanced in the future.

## 566 Supporting information

567 **S1 Text.** Supporting information for Efficient and Flexible Integration of Variant Characteristics  
568 in Rare Variant Association Studies Using Integrated Nested Laplace Approximation

## 569 Funding

570 This project has received funding from the European Union’s H2020 research and innovation  
571 programme under grant agreement No 635290 (PanCanRisk). We also acknowledge support of  
572 the Generalitat de Catalunya’s PERIS program (SLT002/16/00310).

## 573 References

574 1. Cohen JC, Kiss RS, Pertsemidis A, Marcel YL, McPherson R, Hobbs HH. Multiple rare  
575 alleles contribute to low plasma levels of HDL cholesterol. *Science* (80- ). 2004;

576 2. Chassaing N, Davis EE, McKnight KL, Niederriter AR, Causse A, David V, et al. Targeted  
577 resequencing identifies PTCH1 as a major contributor to ocular developmental anomalies

578 and extends the SOX2 regulatory network. *Genome Res.* 2016;

579 3. Priest JR, Osoegawa K, Mohammed N, Nanda V, Kundu R, Schultz K, et al. De Novo  
580 and Rare Variants at Multiple Loci Support the Oligogenic Origins of Atrioventricular  
581 Septal Heart Defects. *PLoS Genet.* 2016;

582 4. Tan PL, Garrett ME, Willer JR, Campochiaro PA, Campochiaro B, Zack DJ, et al. Systematic functional testing of rare variants: Contributions of CFI to age-related macular  
583 degeneration. *Investig Ophthalmol Vis Sci.* 2017;

585 5. Tennessen JA, Bigham AW, O 'connor TD, Fu W, Kenny EE, Gravel S, et al. Evolution  
586 and Functional Impact of Rare Coding Variation from Deep Sequencing of Human  
587 Exomes Broad GO, Seattle GO, on behalf of the NHLBI Exome Sequencing Project.  
588 *Science* (80- ). 2012;

589 6. Nelson MR, Wegmann D, Ehm MG, Kessner D, St. Jean P, Verzilli C, et al. An  
590 abundance of rare functional variants in 202 drug target genes sequenced in 14,002  
591 people. *Science* (80- ). 2012;

592 7. Zuk O, Schaffner SF, Samocha K, Do R, Hechter E, Kathiresan S, et al. Searching for  
593 missing heritability: Designing rare variant association studies. *Proc Natl Acad Sci.* 2014;

594 8. Li B, Leal SM. Methods for Detecting Associations with Rare Variants for Common  
595 Diseases: Application to Analysis of Sequence Data. *Am J Hum Genet.* 2008;

596 9. Price AL, Kryukov G V., de Bakker PIW, Purcell SM, Staples J, Wei LJ, et al. Pooled  
597 Association Tests for Rare Variants in Exon-Resequencing Studies. *Am J Hum Genet.*  
598 2010;

599 10. Madsen BE, Browning SR. A groupwise association test for rare mutations using a  
600 weighted sum statistic. *PLoS Genet.* 2009;

601 11. Liu DJ, Leal SM. A novel adaptive method for the analysis of next-generation sequencing  
602 data to detect complex trait associations with rare variants due to gene main effects and  
603 interactions. *PLoS Genet.* 2010;

604 12. Wu MC, Lee S, Cai T, Li Y, Boehnke M, Lin X. Rare-variant association testing for  
605 sequencing data with the sequence kernel association test. *Am J Hum Genet.* 2011;

606 13. Neale BM, Rivas MA, Voight BF, Altshuler D, Devlin B, Orho-Melander M, et al. Testing  
607 for an unusual distribution of rare variants. *PLoS Genet.* 2011;

608 14. Moutsianas L, Agarwala V, Fuchsberger C, Flannick J, Rivas MA, Gaulton KJ, et al. The  
609 Power of Gene-Based Rare Variant Methods to Detect Disease-Associated Variation and  
610 Test Hypotheses About Complex Disease. *PLoS Genet.* 2015;

611 15. Lee S, Wu MC, Lin X. Optimal tests for rare variant effects in sequencing association  
612 studies. *Biostatistics.* 2012;

613 16. He L, Pitkäniemi J, Sarin AP, Salomaa V, Sillanpää MJ, Ripatti S. Hierarchical bayesian  
614 model for rare variant association analysis integrating genotype uncertainty in human  
615 sequence data. *Genet Epidemiol.* 2015;

616 17. Sun J, Zheng Y, Hsu L. A Unified Mixed-Effects Model for Rare-Variant Association in  
617 Sequencing Studies. *Genet Epidemiol.* 2013;

618 18. Rue H, Martino S, Chopin N. Approximate Bayesian inference for latent Gaussian models  
619 by using integrated nested Laplace approximations. *J R Stat Soc Ser B Stat Methodol.*

620 2009;

621 19. Cowles MK, Carlin BP. Markov Chain Monte Carlo Convergence Diagnostics: A  
622 Comparative Review. *J Am Stat Assoc.* 1996;

623 20. Rue Hå, Martino S. Approximate Bayesian inference for hierarchical Gaussian Markov  
624 random field models. *J Stat Plan Inference.* 2007;

625 21. Martins TG, Simpson D, Lindgren F, Rue H. Bayesian computing with INLA: New  
626 features. *Comput Stat Data Anal.* 2013;

627 22. Blangiardo M, Cameletti M, Baio G, Rue H. Spatial and spatio-temporal models with R-  
628 INLA. *Spatial and Spatio-temporal Epidemiology.* 2013.

629 23. Tierney L, Kadane JB. Accurate approximations for posterior moments and marginal  
630 densities. *J Am Stat Assoc.* 1986;

631 24. Spiegelhalter DJ, Best NG, Carlin BP, Van Der Linde A. Bayesian measures of model  
632 complexity and fit. *J R Stat Soc Ser B Stat Methodol.* 2002;

633 25. Holand AM, Steinsland I, Martino S, Jensen H. Animal Models and Integrated Nested  
634 Laplace Approximations. *G3&#38; Genes|Genomes|Genetics.* 2013;

635 26. Abecasis G, Altshuler D, A A, Brooks L, RM D, Gibbs R, et al. A map of human genome  
636 variation from population scale sequencing. *Nature.* 2010;

637 27. 1000 Genomes Project Consortium, Auton A, Brooks LD, Durbin RM, Garrison EP, Kang  
638 HM, et al. A global reference for human genetic variation. *Nature.* 2015;

639 28. So HC, Gui AHS, Cherny SS, Sham PC. Evaluating the heritability explained by known

640 susceptibility variants: A survey of ten complex diseases. *Genet Epidemiol.* 2011;

641 29. Ferlay J, Steliarova-foucher E, Lortet-tieulent J, Rosso S. Cancer incidence and mortality

642 patterns in Europe : Estimates for 40 countries in 2012. *Eur J Cancer.* 2013;

643 30. Hudson TJ, Anderson W, Aretz A, Barker AD, Bell C, Bernabé RR, et al. International

644 network of cancer genome projects. *Nature.* 2010.

645 31. Puente XS, Beà S, Valdés-Mas R, Villamor N, Gutiérrez-Abril J, Martín-Subero JI, et al.

646 Non-coding recurrent mutations in chronic lymphocytic leukaemia. *Nature.* 2015;

647 32. Muyas F, Bosio M, Puig A, Susak H, Domènech L, Escaramis G, et al. Allele balance

648 bias identifies systematic genotyping errors and false disease associations. *Hum Mutat.*

649 2019;

650 33. Alves-Silva JC, de Carvalho JL, Rabello DA, Serejo TRT, Rego EM, Neves FAR, et al.

651 GLP overexpression is associated with poor prognosis in Chronic Lymphocytic Leukemia

652 and its inhibition induces leukemic cell death. *Invest New Drugs. Investigational New*

653 *Drugs;* 2018;36(5):955–60.

654 34. Li Y, Brown P, Rue H, Al-Maini M, Fortin P. Spatial modelling of lupus incidence over 40

655 years with changes in census areas. *J R Stat Soc Ser C Appl Stat.* 2012;

656 35. Ruiz-Cárdenas R, Krainski ET, Rue H. Direct fitting of dynamic models using integrated

657 nested Laplace approximations - INLA. *Comput Stat Data Anal.* 2012;

658 36. Martino S, Aas K, Lindqvist O, Neef LR, Rue H. Estimating stochastic volatility models

659 using integrated nested laplace approximations. *Eur J Financ.* 2011;

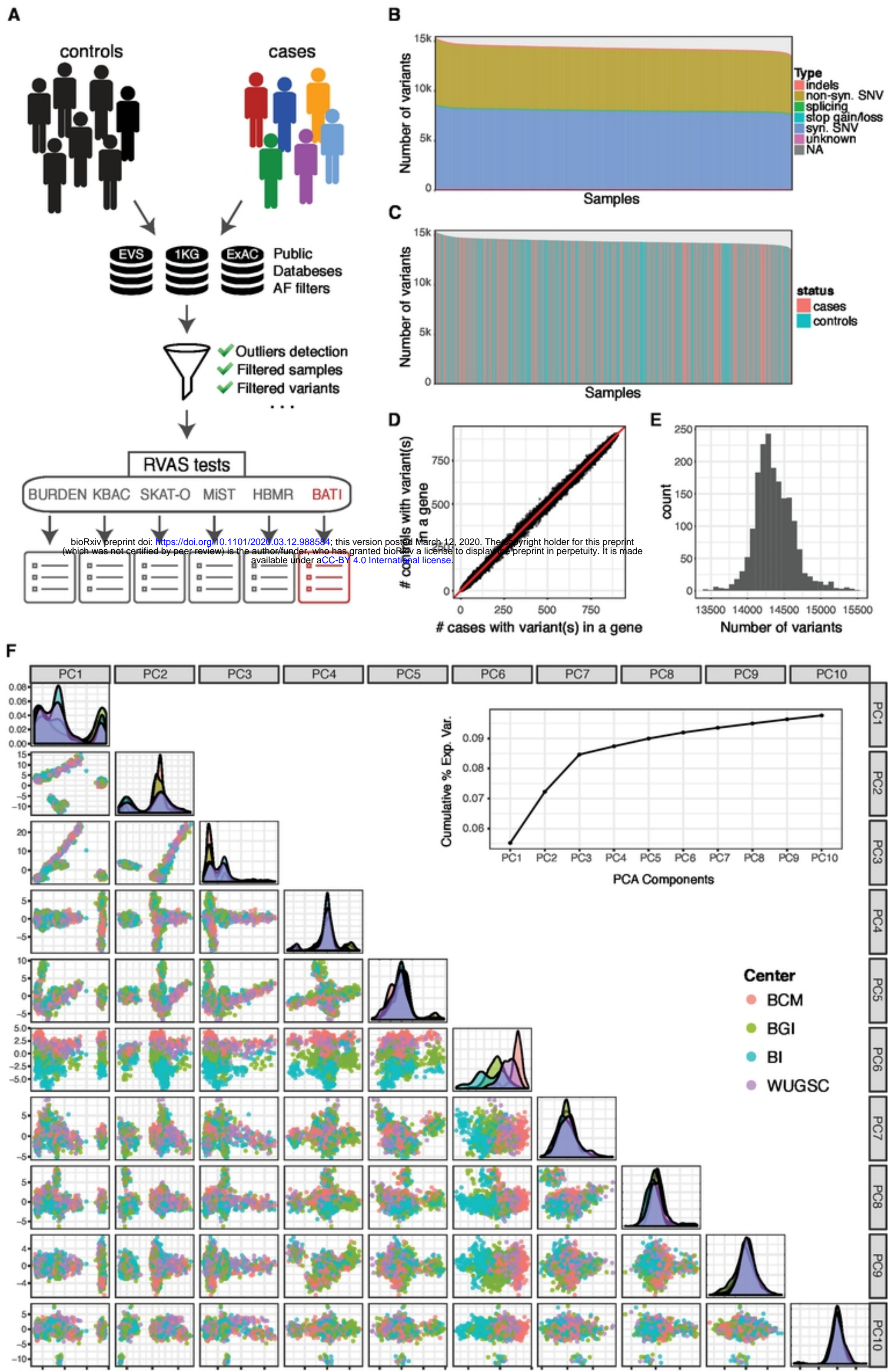
660 37. Roos M, Held L. Sensitivity analysis in Bayesian generalized linear mixed models for

661 binary data. *Bayesian Anal.* 2011;

662 38. Schrödle B, Held L, Riebler A, Danuser J. Using integrated nested Laplace  
663 approximations for the evaluation of veterinary surveillance data from Switzerland: A  
664 case-study. *J R Stat Soc Ser C Appl Stat.* 2011;

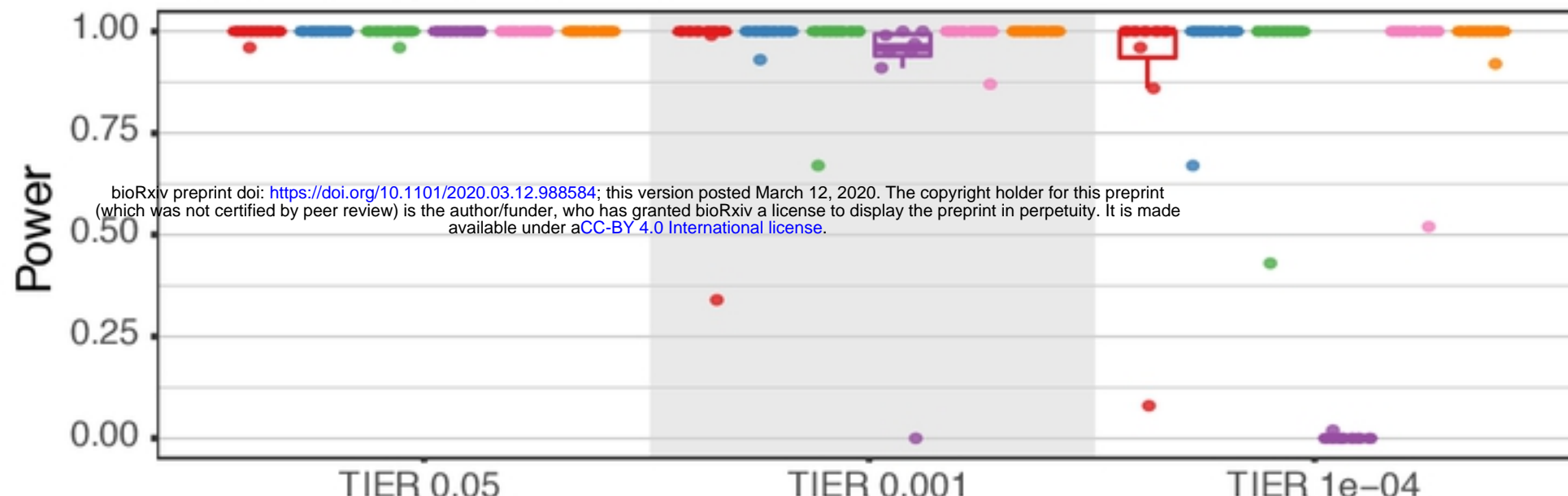
665 39. Paul M, Riebler A, Bachmann LM, Rue H, Held L. Bayesian bivariate meta-analysis of  
666 diagnostic test studies using integrated nested Laplace approximations. *Stat Med.* 2010;

667

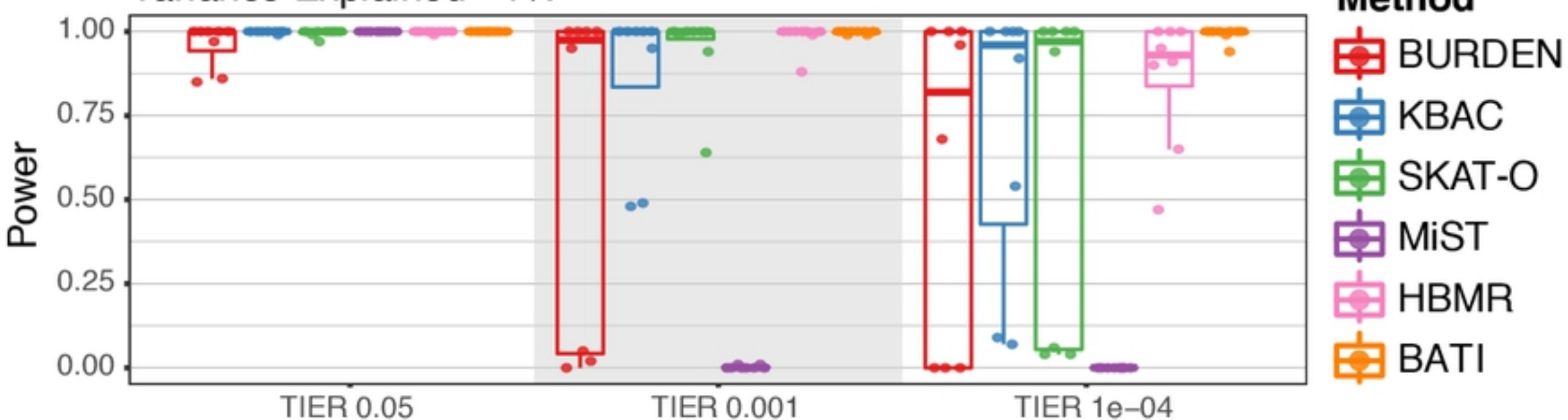


Figure

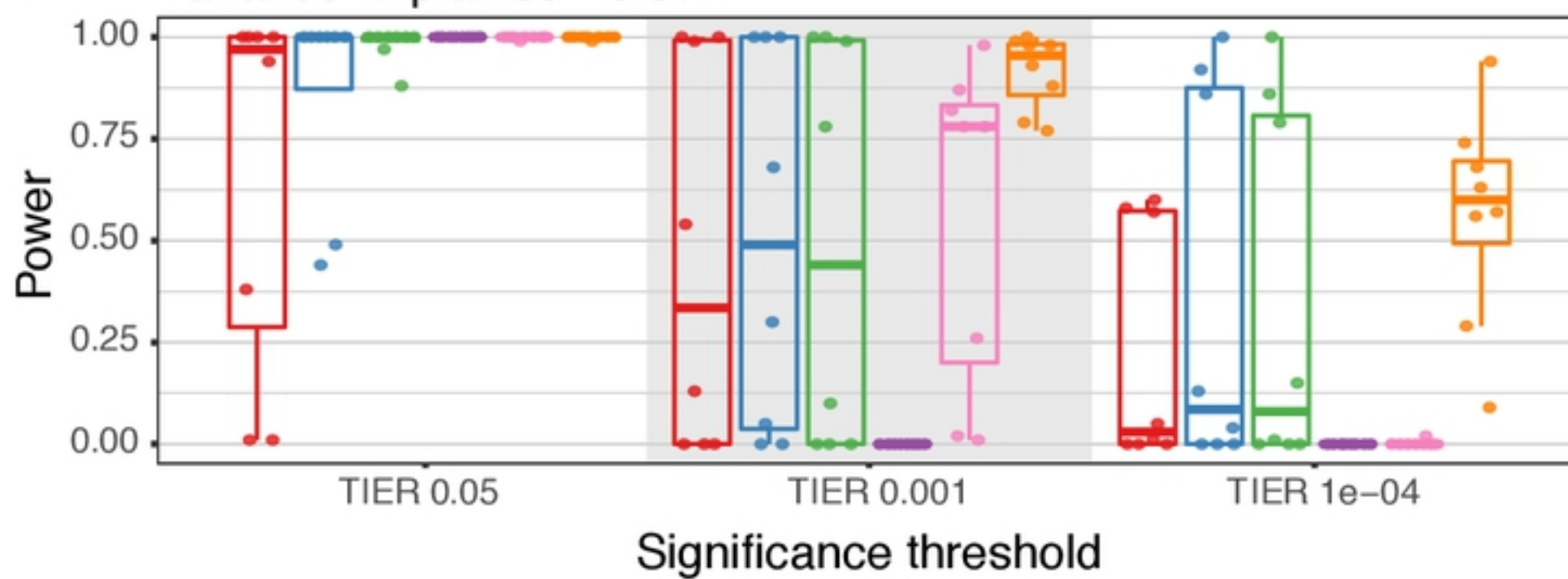
### A Variance Explained ~2%



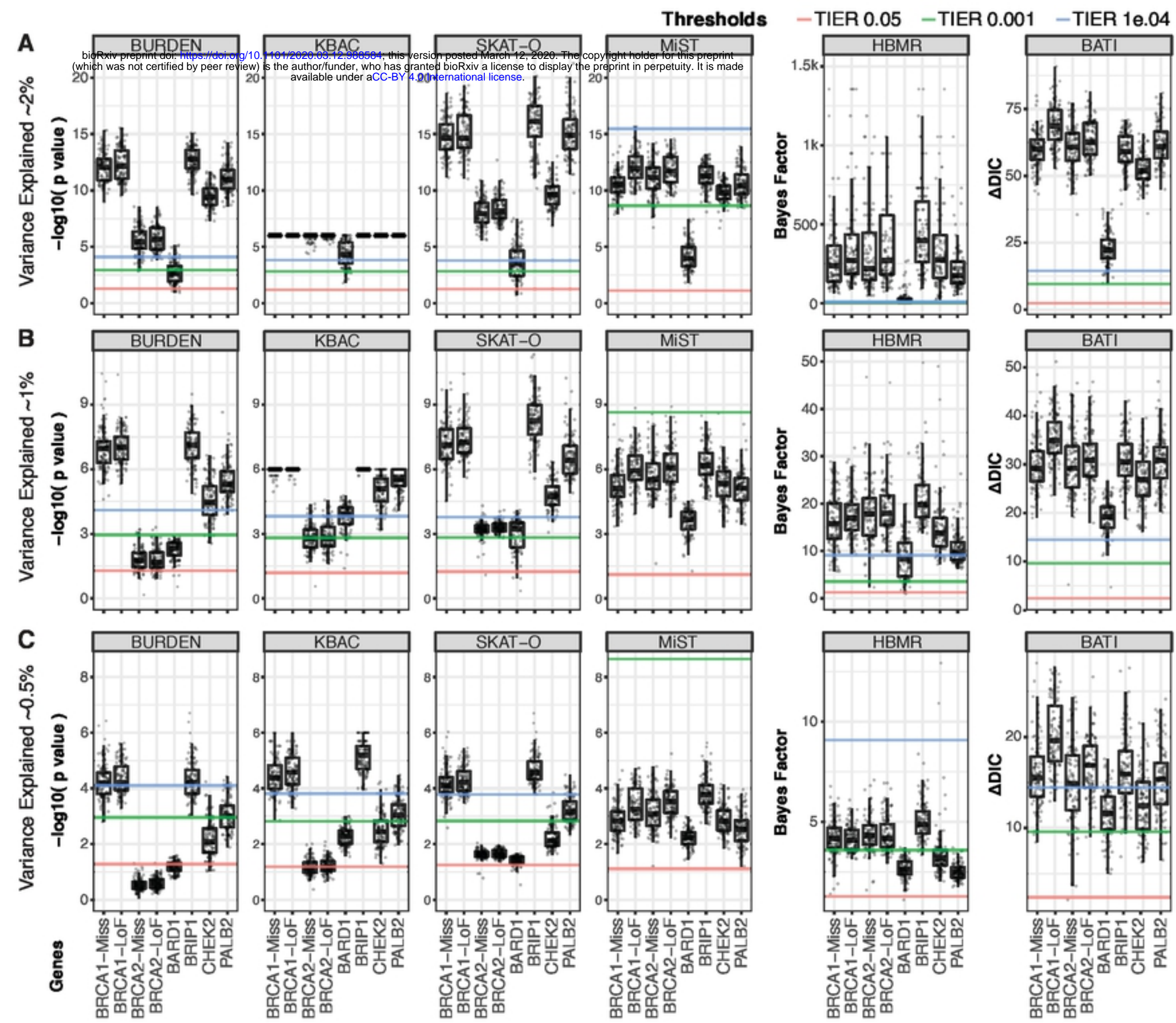
### B Variance Explained ~1%



### C Variance Explained ~0.5%



Figure



Figure